Geoderma 232–234 (2014) 437–448

Contents lists available at ScienceDirect

Geoderma

journal homepage: www.elsevier.com/locate/geoderma

Evaluation of a model framework to estimate soil and soil organic carbon redistribution by water and tillage using ^{137}Cs in two U.S. Midwest agricultural fields

Claudia J. Young [a,b,*], Shuguang Liu [b], Joseph A. Schumacher [c], Thomas E. Schumacher [c], Thomas C. Kaspar [d], Gregory W. McCarty [e], Darrell Napton [c], Dan B. Jaynes [d]

[a] ERT Inc., contractor to the U.S. Geological Survey (USGS) Earth Resources Observation and Science (EROS) Center, Sioux Falls, SD 57198, USA
[b] USGS EROS Center, Sioux Falls, SD 57198, USA
[c] South Dakota State University, Brookings, SD 57007, USA
[d] USDA-ARS National Laboratory for Agriculture and the Environment, Ames, IA 50011, USA
[e] USDA-ARS Hydrology and Remote Sensing Laboratory, Beltsville, MD 20705, USA

ARTICLE INFO

Article history:
Received 21 October 2013
Received in revised form 21 May 2014
Accepted 24 May 2014
Available online xxxx

Keywords:
Erosion
Deposition
Water erosion
Tillage
Cs-137
Organic carbon

ABSTRACT

Cultivated lands in the U.S. Midwest have been affected by soil erosion, causing soil organic carbon (SOC) redistribution in the landscape and other environmental and agricultural problems. The importance of SOC redistribution on soil productivity and crop yield, however, is still uncertain. In this study, we used a model framework, which includes the Unit Stream Power-based Erosion Deposition (USPED) and the Tillage Erosion Prediction (TEP) models, to understand the soil and SOC redistribution caused by water and tillage erosion in two agricultural fields in the U.S. Midwest. This model framework was evaluated for different digital elevation model (DEM) spatial resolutions (10-m, 24-m, 30-m, and 56-m) and topographic exponents ($m = 1.0$–1.6 and $n = 1.0$–1.3) using soil redistribution rates from ^{137}Cs measurements. The results showed that the aggregated 24-m DEM, $m = 1.4$ and $n = 1.0$ for rill erosion, and $m = 1.0$ and $n = 1.0$ for sheet erosion, provided the best fit with the observation data at both sites. Moreover, estimated average SOC redistributions were 1.3 ± 9.8 g C m^{-2} yr^{-1} in field site 1 and 3.6 ± 14.3 g C m^{-2} yr^{-1} in field site 2. Spatial distribution patterns showed SOC loss (negative values) in the eroded areas and SOC gain (positive value) in the deposition areas. This study demonstrated the importance of the spatial resolution and the topographic exponents to estimate and map soil redistribution and the SOC dynamics throughout the landscape, helping to identify places where erosion and deposition from water and tillage are occurring at high rates. Additional research is needed to improve the application of the model framework for use in local and regional studies where rainfall erosivity and cover management factors vary. Therefore, using this model framework can help to improve the information about the spatial distribution of soil erosion across agricultural landscapes and to gain a better understanding of SOC dynamics within eroding and previously eroded fields.
© 2014 Elsevier B.V. All rights reserved.

1. Introduction

Projected global warming and degradation of land resources by erosion are critical environmental challenges (Jacinthe and Lal, 2007). Soil erosion is a natural process; however, it can be accelerated by human activities, such as intensive and conventional agricultural practices. Furthermore, soil erosion can become a major environmental and agricultural problem and cause reductions in soil productivity and deterioration of water and air quality (Pimentel et al., 1995; USDA NRCS, 1997). Erosion is defined as the detachment or movement of soil caused by water, wind, or human activities (e.g., tillage operations). The magnitude of erosion, however, is mostly determined by rainfall intensity, soil type, ground cover, and landscape characteristics (Arriaga and Lowery, 2007; Flanagan, 2007; Römkens et al., 2002). Soil erosion can have several effects on crop yield and soil productivity, including reductions in effective rooting depth, available nutrients and water for plants, and loss of surface soil structure and infiltration due to exposure of subsoil (Schumacher, 2007). Water erosion consists of three recognized types: sheet, rill, and gully (Brady and Weil, 2008). Sheet erosion occurs when raindrops impact the soil surface, uniformly dislodging soil particles in the top soil layer (Brady and Weil, 2008; Nelson, 2002; Pimentel, 2006). Rill erosion, which is especially common on bare land, happens as the sheet flow is concentrated into small channels (Brady and Weil, 2008). Gully erosion occurs when runoff is further concentrated, cutting deeper into the soil and creating larger channels that can become an obstacle for machinery operations (Brady and Weil, 2008). Tillage erosion can be defined as the

* Corresponding author at: ERT, Inc. at USGS EROS Center, 47914 252nd Street, Sioux Falls, SD 57198, USA.
E-mail address: cyoung@usgs.gov (C.J. Young).

http://dx.doi.org/10.1016/j.geoderma.2014.05.019
0016-7061/© 2014 Elsevier B.V. All rights reserved.

downslope displacement of soil through the actions of tillage operations and gravity (Lindstrom, 2007). The location of soil erosion and deposition zones along the hillslope is dependent on the erosion process and hillslope characteristics. Net soil loss from water erosion occurs in the mid to lower back-slope positions primarily as a result of concentrated flow in rills, while soil displacement resulting from tillage erosion occurs primarily on shoulder positions. Hence, a mix of erosion processes is likely to occur on most landscapes with complex slope configurations (Schumacher et al., 1999).

In the United States, soil erosion on agricultural lands is one of the major causes of land degradation and water quality deterioration (Blanco and Lal, 2008; Nelson, 2002). Model estimates have shown that the rate of total erosion has declined since the 1970s (Blanco and Lal, 2008) because of federal regulations and guidelines, such as the Soil and Water Conservation Act of 1977 and the Food Security Act of 1985 ("Farm Bill"), aimed at controlling soil erosion and sediment delivery to streams and rivers (Toy et al., 2002). Despite this declining rate, erosion is still a serious problem in the United States—about one-third of U.S. croplands have continued eroding and losing topsoil at increasingly rapid rates (Blanco and Lal, 2008). The intensively cultivated and cropped lands that produce corn and soybean in the U.S. Midwest have been particularly affected by soil erosion (Schmidt and Ham, 1999). For example, Pimentel (2006) argued that one-half of the fertile topsoil in Iowa has been lost through erosion during the last 150 years of farming, and erosion continues today at a rate of about 30 t ha^{-1} yr^{-1} because of the rolling topography and the type of agricultural practices. One of these practices, moldboard plowing, which inverts the soil and buries the residue, was widely used in the Midwest and was thought to have contributed substantially to erosion and reduction of soil organic carbon (SOC) in croplands (Olson, 2013). Conversely, other management practices, such as no-till, conservation tillage, buffer strips, and terraces, have been applied to reduce erosion and loss of SOC. For example, conservation tillage systems have been proposed as one way to sequester 0.50 Mg ha^{-1} yr^{-1} of C in agricultural soil in the United States (Lal, 1998).

SOC plays a considerable and unique role in the global carbon (C) cycle because it is part of the total soil carbon pool of about 2300 Pg, which is three times the atmospheric pool (770 Pg) and 3.8 times the biotic pool (620 Pg) (Lal, 2002). Ito (2007) argued that SOC displacement by erosion may have a considerable impact on terrestrial carbon storage and that water erosion will be strongly influenced by future climate change and land use activities in many regions of the world. In addition, Smith et al. (2005) and Liu et al. (2003) showed that erosion can redistribute SOC within a landscape, moving soil and SOC from upland sites and depositing this eroded soil and SOC into lowland areas. Therefore, soil erosion may be a dominant force in the redistribution of SOC within agricultural landscapes, and this redistribution may impact C oxidation or sequestration (McCarty and Ritchie, 2002). However, the effect of soil redistribution from erosion on SOC dynamics is still uncertain. Some studies have shown that agricultural erosion can act as an important stimulant of CO_2 emissions (Lal, 2003; Lal and Pimentel, 2008), promote C sequestration (Harden et al., 2008; Liu et al., 2003; Smith et al., 2005), or do both (Van Oost et al., 2007).

Modeling soil erosion is the process of mathematically describing soil particle detachment, transport, and deposition on land surfaces. The goals of erosion models are to (1) simulate the total detachment and movement of soil particles caused by rainfall, runoff, and tillage in an area, (2) predict soil loss or gain for a specific area, (3) estimate the hazard or risk associated with the removal of topsoil, both onsite (fertility loss, gullying) and offsite (muddy floods and downstream pollution), and (4) simulate the effects on erosion of a change in land use, application of soil conservation measures, or a change in climate (Jetten and Maneta, 2010).

Three types of models have usually been used to simulate soil erosion: empirical, physically-based, and conceptual (Nearing et al., 1994). An example of an empirical model is the Tillage Erosion Prediction (TEP) developed by Lindstrom et al. (2000). Additionally, stream power models have become standard for large-scale erosion modeling in geographic information systems (GIS) (Mitas and Mitasova, 1998), such as the Unit Stream Power-based Erosion Deposition (USPED) model developed by Mitasova et al. (1996). In GIS-based erosion models, the choice of digital elevation model (DEM), resolution, and flow routing may vary the quality of the output (Wilson and Lorang, 2000). For example, several studies have indicated that DEM cell size can affect the modeling of landscapes with complex terrain (Claessens et al., 2005; Schoorl et al., 2000; Zhang et al., 2009).

When modeling erosion, calibration and validation are important components for model evaluation. Calibration helps to improve the predictive quality and usefulness of models (Jetten and Maneta, 2010). Validation can verify that the model is rational and can give reasonable prediction when compared with observed information (Morgan, 2010), and it can be applied in different areas. Jetten and Maneta (2010) noted that model validation is often ignored in many modeling studies after calibration has been completed. Regardless of the model type used for modeling soil redistribution, calibration and validation require field measurements of erosion and deposition.

Over the past 50 years, the use of natural and non-natural radioisotopes to study erosion and sedimentation has drawn considerable attention. Cesium-137 (^{137}Cs) is one of the non-natural radioisotopes introduced into the atmosphere from nuclear weapons tests in the 1950s and 1960s. This radionuclide moves from the stratosphere back to the earth's surface (fallout) where it is strongly absorbed by soil particles, so it is a unique tracer for erosion and sedimentation in terrestrial systems over a broad range of spatial and temporal scales (Fang et al., 2012; Fornes et al., 2005; Ritchie and McHenry, 1990). Recently, many studies have used ^{137}Cs to assess soil and SOC redistribution and to find spatial patterns across agricultural landscapes (Fornes et al., 2005; Ritchie and McHenry, 1990; Ritchie et al., 2007; Schumacher et al., 2005; Van Oost et al., 2007; Warren et al., 2005).

The main objective of this study was to evaluate a soil modeling framework and to estimate and understand the soil and SOC redistribution caused by water and tillage erosion in two agricultural fields in Iowa of the U.S. Midwest where corn–soybean rotation and different tillage practices have been applied since about 1957. Specific objectives of this study were to (1) calibrate and validate the model framework, which includes the USPED and the TEP models, using different DEM cell size and topographic parameters, (2) evaluate simulated results with observed information from ^{137}Cs measurements, and (3) estimate SOC redistribution to assess carbon gain and loss from erosion and deposition by water and tillage.

2. Materials and methods

For this study, a model framework was used to understand the spatial distribution of soil and SOC caused by water and tillage erosion. This model framework consisted of two models: USPED and TEP. The models required different information including precipitation, soil, topography, land use and land cover, and management, which was collected in a related study by Schumacher et al. (2005). In this study, the DEM cell size was evaluated in two field sites (field sites 1 and 2). Based on these results, the best fit was selected to calibrate the topographic parameters in field site 1. The simulated estimates of soil redistribution (erosion and deposition) rates for each of the possible combinations of the calibrated parameters were compared with those derived from ^{137}Cs measurements by Ritchie et al. (2007) and used by Schumacher et al. (2005). The topographic parameters with the best fit in field site 1 were used in field site 2 to validate the model framework. The results from each site were then used to estimate SOC redistribution.

2.1. Study area

Two agricultural fields in Iowa were selected for this study, where different studies and measurements had been conducted, including

elevation mapping, yield variability, soil mapping, farming system comparisons, and ^{137}Cs measurements (Colvin et al., 1997; Karlen and Colvin, 1992; Kaspar et al., 2004; Ritchie et al., 2007; Schumacher et al., 2005; Steinwand et al., 1996). These two Iowa farm fields are located in the Des Moines Lobe Till Plain in central Iowa near Ames, and each has an area of about 15 ha (Fig. 1). Mean annual precipitation is about 835 mm and mean annual temperature is approximately 8 °C, ranging from −6 °C in January to 22 °C in July; soil types are Hapludolls, Endoaquolls, and Calciaquolls; and both fields have tile drains with no surface inlets (Ritchie et al., 2007). The native vegetation in the study areas is tallgrass prairie (Weaver, 1920). In addition, the fields are in a corn and soybean rotation, alternating each year.

The first study field (field site 1) is located between Boone and Ames, IA (Fig. 1). This field site is characterized by low relief swell and swale topography with poorly developed surface drainage (Kaspar et al., 2004). Moreover, conventional farming practices have been applied since 1932. A corn–oats–hay rotation was applied from 1932 to 1957, then a corn–soybean rotation from 1957 to present. Tillage practices in this field were fall moldboard plowing followed by spring disking and harrowing between 1932 and 1981; after 1982 fall chisel plowing or disking followed by spring harrowing has been the primary tillage practice; in recent years fall tillage after soybean harvest was replaced by two disking or harrowing operations in the spring before corn planting (Karlen and Colvin, 1992; Kaspar et al., 2004; Schumacher et al., 2005). Elevation at this field site, based on measurements with a kinematic differential global position system receiver, ranges from 293 to 296 m with an average and standard deviation of about 294 ± 0.8 m (Fig. 2a). Percent slope, derived from the elevation, ranges from 0.13 to 5.4% with an average and standard deviation of about 2 ± 1.1% (Fig. 2c).

The second study field (field site 2) is located in an agricultural area south of Ames, IA (Fig. 1). The management practices have been similar to field site 1, including corn–soybean rotation and moldboard plowing in the fall after corn (even years) and fall chisel plowing after soybean (odd years), with one or two field cultivator passes in the spring before planting and one row cultivation during summer before 1992. Management after 1992 continued to be the same except for replacing fall moldboard plowing with fall chisel plowing (Al-Smadi, 2007). Hence, in this study, the cover and management factor (C_f) for crop and tillage practices was assumed to be the same for both field sites. The elevation in this field site, measured with the same methods as field site 1, ranges from 312 to 316 m with an average and standard deviation of 313 ± 1 m (Fig. 2b). Percent slope derived from the elevation ranges from 0 to 9.6% with an average and standard deviation of 2.6 ± 1.7% (Fig. 2d).

2.2. Model framework

Fig. 3 shows a flow diagram of the model framework used in this study, including inputs and outputs. This model framework was built using Python programming language, ArcGIS desktop with the geoprocessing module for Python (Esri, 2011), and the R statistical package scripts (R Development Core Team, 2010).

2.2.1. Unit Stream Power-based Erosion Deposition (USPED) Model

The USPED model is a two-dimensional model that predicts the spatial distribution of soil erosion and deposition for a steady state overland flow with uniform rainfall excess conditions for a transport capacity limited case of the erosion process (Mitas and Mitasova, 1998; Mitasova et al., 1996). The USPED model is an improvement over the one-dimensional Universal Soil Loss Equation (USLE) and the Revised USLE (RUSLE) models because it accounts for deposition using four of the one-dimension model factors (R_f, K_f, C_f, P_f) and flow convergence, which is calculated based on upslope contributing area (Liu et al., 2007; Mitasova et al., 1996). Therefore, the sediment transport capacity (T) is defined in the following equation (Eq. (1)):

$$T = R_f \times K_f \times C_f \times P_f \times A^m \times (\sin\beta)^n \quad (1)$$

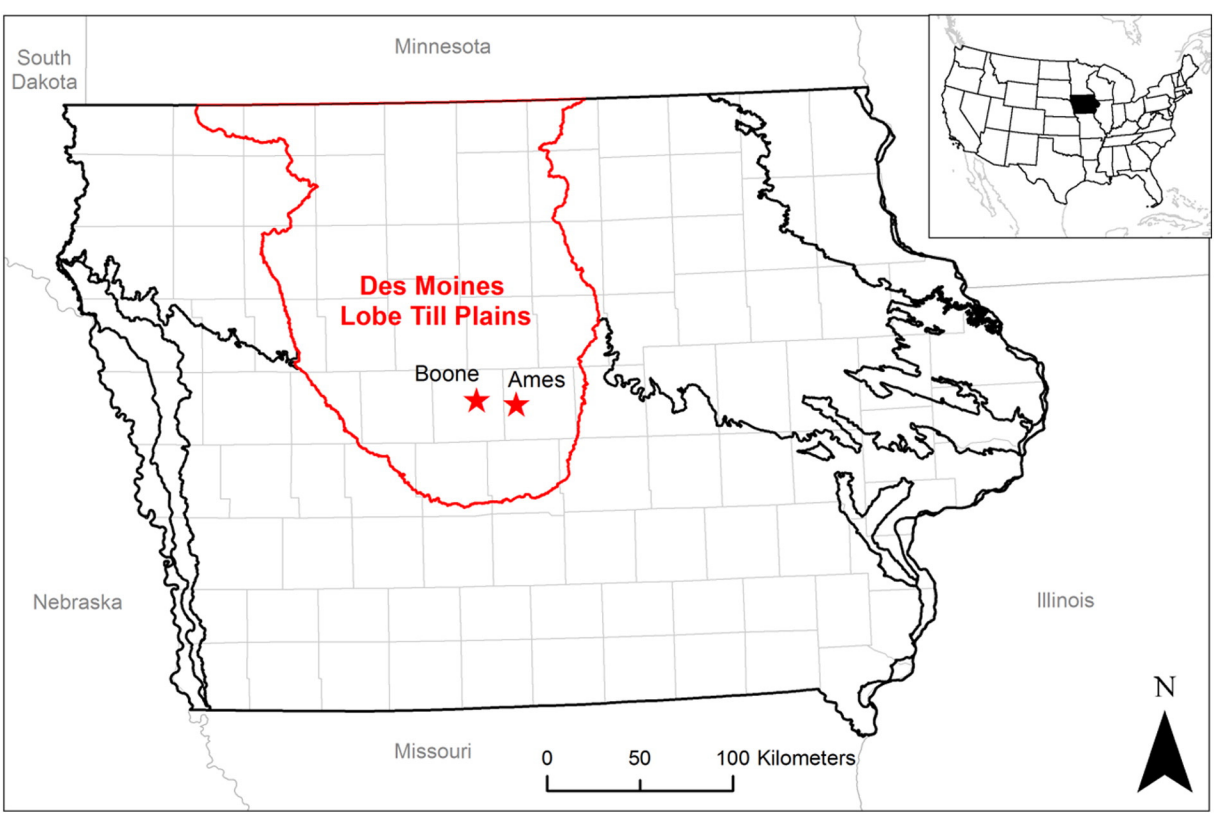

Fig. 1. Location of the Des Moines Lobe Till Plains, Boone and Ames in Iowa where the study sites (field sites 1 and 2) are found.

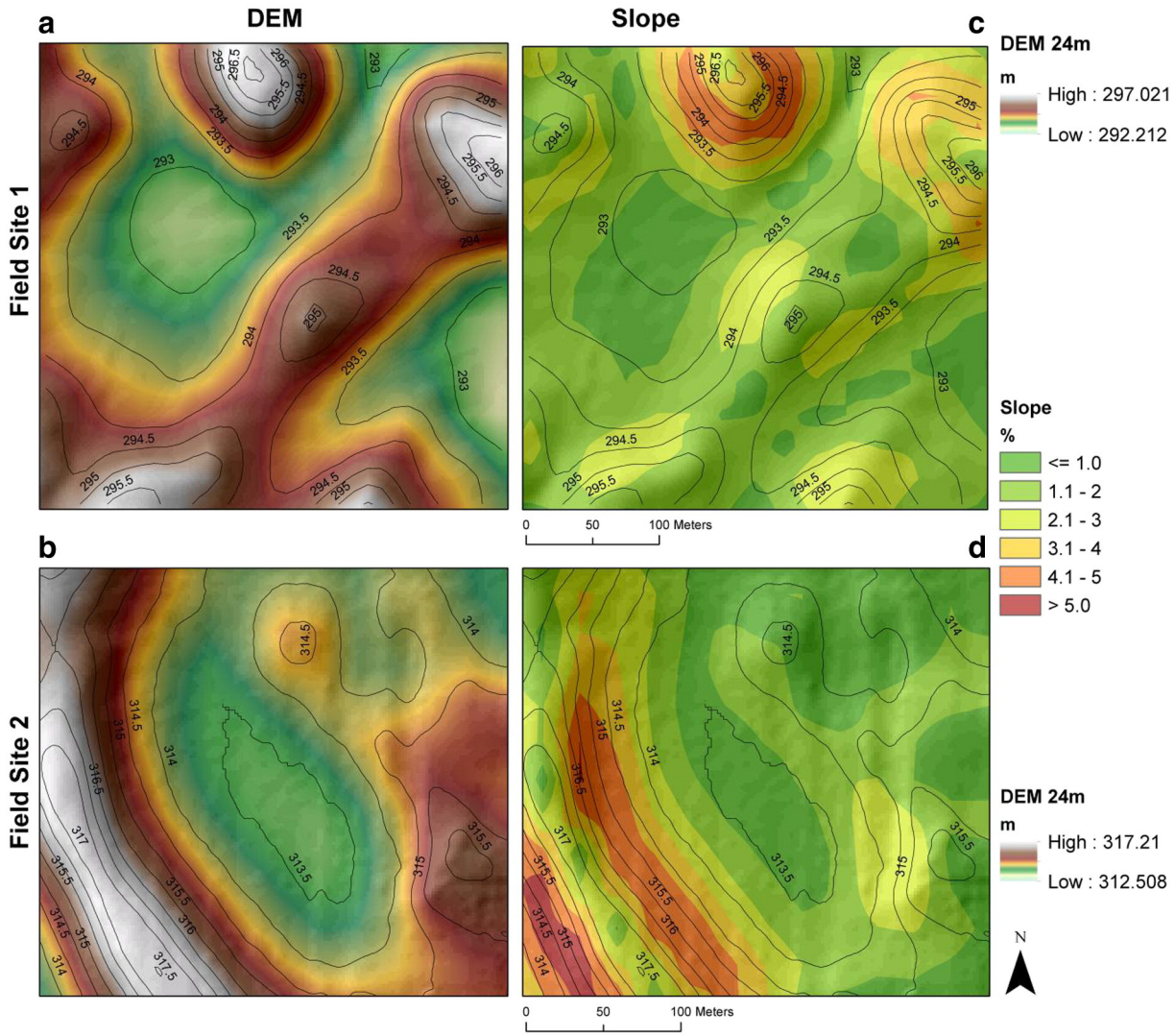

Fig. 2. Digital elevation model (DEM) (a and b) and percentage of slope (c and d) along with contour lines for every 0.5 m and hillshade, derived from the DEM, in the two field study areas in Iowa: (a and c) field site 1 and (b and d) field site 2.

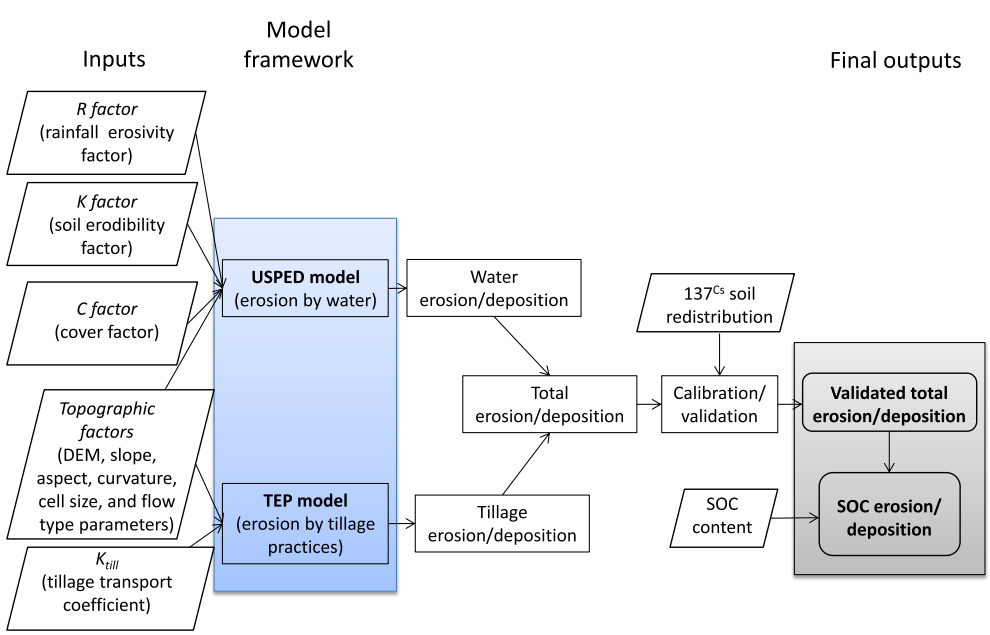

Fig. 3. Flow diagram of the model framework used in this study, including inputs and outputs.

where R_f is the rainfall factor, K_f is the soil erodibility factor, C_f is the cover and management factor, P_f is the conservation practice factor, A is the upslope contributing area, and β is the slope inclination angle in degrees. The exponents m and n control the relative impact of water and slope terms and reflect different erosion patterns for different types of flow (rill or sheet erosion), where $m = 1.0$–1.6 and $n = 1.0$–1.3. Previous studies have used the recommended $m = 1.6$ and $n = 1.3$ for rill erosion and $m = 1.0$ and $n = 1.0$ for sheet erosion (Garcia Rodriguez and Gimenez Suarez, 2012; Liu et al., 2007; Warren et al., 2005). However, these exponents can be calibrated if data are available for a specific prevailing type of flow and soil conditions (Leh et al., 2011; Mitasova and Mitas, 2001; Mitasova et al., 1999). For this study, a modification of the upslope contributing area calculation was applied, where m and n values increased as percent of slope increased. This approach is used by the Integrated Valuation of Environmental Services and Tradeoff (InVEST) model for the topographic (LS) factor calculation in the USLE equation for the sediment retention model (Tallis et al., 2011). Then, based on T in Eq. (1), erosion and deposition (ED) can be calculated using the divergence equation according to Mitas and Mitasova (1998) as a change in sediment flow rate expressed by a divergence in the sediment flow (Eq. (2)):

$$ED = \frac{d(T \times \cos a)}{dx} + \frac{d(T \times \sin a)}{dy} \tag{2}$$

where a, the aspect of the elevation surface, and $dx = dy$, the grid resolution, are used to determine contribution area upstream (Oliveira et al., 2013). Simulation results from the USPED model can be positive, indicating soil deposition, or negative, indicating soil erosion. To be consistent with units in the model framework, the USPED results were converted from tons per acre per year (tons acre^{-1} yr^{-1}) to metric tons per hectare per year (t ha^{-1} yr^{-1}) based on Foster et al. (1981).

2.2.2. Tillage Erosion Prediction (TEP) model

Soil movement from tillage operations also has been identified as a cause of soil erosion (Lindstrom et al., 2000). Tillage erosion is a problem that has been present since the dawn of cultivation, and evidence of tillage erosion is commonly observed as a difference in soil color between hilltops and adjacent lower slope positions (Lindstrom, 2007). A simple model developed by Lindstrom et al. (2000) can be used to describe the soil redistribution along a hillslope transect in cultivated fields that results from tillage action. The tillage erosion prediction (TEP) model is based on Eq. (3):

$$k_{till} = -D\rho_b B \tag{3}$$

where k_{till} is the tillage transport coefficient (kg m^{-1}), D is the depth of tillage (m), ρ_b is the soil bulk density (kg m^{-3}), and B is the average soil displacement (m) as a function of the slope gradient (m m^{-1}). This model estimates the net soil movement for individual hillslope segments across a field transect for individual tillage operations (Lindstrom et al., 2000). Therefore, this model can identify areas, based on landscape configuration, of excessive soil loss (erosion) or gain (deposition) caused by tillage operations. A geographic information system (GIS) implementation of the TEP model by Lindstrom et al. (2000) provides relative values that describe varying tillage erosion potential at the field scale. In this GIS approach, two-dimensional tillage erosion values are determined with a simplified equation:

$$ED_{till} = \left[k_{till} \times \left(\frac{(S_E - S_W)}{\Delta x}\right) + k_{till} \times \left(\frac{(S_S - S_N)}{\Delta x}\right)\right] \times 10 \tag{4}$$

where Δx is the distance (m) between the midpoints of two consecutive slope segments on a projected grid (N–S and E–W vectors), S is the slope gradient (m m^{-1}) which is positive in the upslope direction and negative in the downslope direction, and k_{till} is the tillage transport coefficient (kg m^{-1}). The estimated tillage erosion rate (ED_{till}) in kg m^{-2} is multiplied by 10 to get results in metric tons per hectare (t ha^{-1}). The two-dimensional tillage erosion estimates using the model in Eq. (4) can be solved using the ArcGIS general curvature tool in the Spatial Analyst extension. These estimates can be calculated by multiplying the DEM general curvature and the k_{till} value. To keep uniformity with the ArcGIS curvature functions in dealing with direction and curvature units and to express tillage erosion in units of metric tons ha^{-1}, the k_{till} value in kg m^{-1} is divided by the negative value of the DEM cell size (m) (e.g., if $k_{till} = 330$ kg m^{-1} and DEM cell size = 10 m, then $k_{till} = -33$). An example of the TEP process for estimating tillage erosion is described in Schumacher et al. (2005).

2.3. Input model settings

Inputs for the models used in this study are summarized in Table 1 for field site 1 and in Table 2 for field site 2. The R and C factors (R_f and C_f) and k_{till} values were based on Schumacher et al. (2005). For the K factor (K_f), the data were extracted from the Soil Survey Geographic (SSURGO) Database (USDA NRCS, 2012). A DEM was derived from elevation and position measurements taken with a kinematic differential global positioning system (DGPS) receiver mounted on an all-terrain vehicle, so that a 2-m regularized DEM was generated using the ArcInfo kriging interpolation tool (Jaynes et al., 2011) (Fig. 2). For this study, the 2-m DEM was aggregated to 10-m, 24-m, 30-m, and 56-m elevation datasets to evaluate the effect of spatial resolution in the model framework. We used the spatial resolution that provided the best fit (R^2) when compared with the ^{137}Cs erosion estimates.

2.4. Fallout ^{137}Cs radionuclide as a soil redistribution tracer

Spatial patterns of ^{137}Cs concentration and mass were measured at the two field study sites, where derived soil redistribution was estimated by Ritchie et al. (2007). Soil samples were collected on a grid pattern across the field using a 3.2-cm-diameter push probe in May 2003 in field site 1 (Schumacher et al., 2005) and in June 2003 in field site 2. The samples were collected for the 0–30-cm layer on a 25-m grid, and deeper soil samples were collected for the 30–50-cm layer at sites of deposition (Ritchie et al., 2005). At least six reference soil samples were collected in undisturbed natural areas where no apparent soil redistribution had occurred since the mid-1950s, and they were used to determine baseline ^{137}Cs input to the field sites. The composite soil samples were dried and analyzed for ^{137}Cs by gamma-ray analysis using a Canberra Genie 2000 Spectroscopy System (Ritchie et al., 2007; Schumacher et al., 2005). Total carbon (%) and nitrogen (%) were measured by dry combustion using a Leco CNS 2000 elemental analyzer on a sub-sample of the dried composited soil sample that was ground to a very fine powder with a roller grinder (Ritchie et al., 2007). Calcium carbonate ($CaCO_3$) was determined by ashing the soil samples in a furnace at 400 °C for 16 h and reanalyzing the ashed sample for the remaining C in $CaCO_3$. SOC was estimated as the difference between total carbon and carbonate carbon (Ritchie et al., 2004). The ^{137}Cs soil redistribution estimates were used as observation data to calibrate and validate the model framework. The calculated SOC content percentage by Ritchie et al. (2007) from each sample location was used to estimate SOC redistribution rates in g C m^{-2} yr^{-1}.

2.5. Model calibration, validation, and evaluation

Model calibration is intended to improve the predictive quality and usefulness of models for their intended purposes or goals. In this study, calibration was applied to the model framework for the different spatial resolutions from a 2-m DEM (10 m, 24 m, 30 m, and 56 m) for both sites and the topographic exponents (m and n) in field site 1 using ^{137}Cs soil redistribution estimates. To evaluate the model framework results, graphical techniques and different statistical analyses and statistics were used. To evaluate the linear association between

Table 1
Input settings used in field site 1.

Input	Value	Units	Source
R factor	150	$\frac{\text{hundreds of ft}-\text{tonf}\cdot\text{in}}{\text{acre}\cdot\text{hr}\cdot\text{yr}}$	Schumacher et al. (2005)
K factor	0.24–0.28	$\frac{\text{ton}\cdot\text{acre}\cdot\text{hr}}{\text{hundreds of acre}\cdot\text{ft}-\text{tonf}\cdot\text{in}}$	SSURGO (USDA NRCS, 2012)
C factor	0.31	Dimensionless	Schumacher et al. (2005)
P factor	1	Dimensionless	Schumacher et al. (2005)
k-till	718	kg m^{-1} yr^{-1}	Schumacher et al. (2005)
DEM	293.9 ± 0.88	m (original spatial resolution 2 m)	Kaspar et al. (2004)
m	1.0–1.6	Dimensionless	Mitasova and Mitas (2001)
n	1.0–1.3	Dimensionless	Mitasova and Mitas (2001)
SOC content	2.24 ± 1.04	Percentage	Ritchie et al. (2007)

DEM: digital elevation model, SOC: soil organic carbon. Value information for DEM and SOC content include mean and standard deviation.

simulated and observed information, a correlation analysis was applied using a 95% confidence interval ($\alpha = 0.05$) to find the best fit of the simulated results with the observed information based on the coefficient of determination (R^2). To evaluate the model framework performance, three quantitative statistics recommended by Moriasi et al. (2007) were included: (1) Nash–Sutcliffe efficiency (NSE), (2) percent bias (PBIAS), and (3) ratio of the root mean square error (RMSE) to the standard deviation of measured data (RSR). Moriasi et al. (2007) considered satisfactory ratings of NSE > 0.5 for simulation trends, RSR ≤ 0.7 for simulation of residual variation, and PBIAS ≤ ±55 for performance in simulation of average of magnitudes for evaluation of model simulation related to sediments in watersheds. Based on these statistics, the DEM cell size was first evaluated in both fields to get the best results; then the topographic combination (*m* and *n*) with the best fit and satisfactory model performance was selected from field site 1 and applied to field site 2 for validation. For observed and predicted datasets from each field site, the Shapiro–Wilk test was applied to test for the normality of the data. If the datasets were non-normal, a Wilcoxon test, a non-parametric test, was applied to compare the model framework predictions and the ^{137}Cs soil redistribution estimates for each field. Graphical techniques used for evaluation included (1) the Taylor Diagram (Taylor, 2001) for the evaluation of the different simulated results from the combinations of topographic exponents with the best fit from the DEM cell size in field site 1, and (2) scatterplots to assess the linear association between the model and ^{137}Cs soil redistribution estimates using the DEM cell size and topographic validated parameters for both field sites.

2.6. Soil organic carbon estimation

Based on the validation process of the model framework in both field sites described in the previous section, the results from each site were used to estimate and evaluate the spatial distribution of SOC redistribution (C mass per unit area). A simple calculation was applied using the simulated net erosion and deposition results with the SOC content measured with the ^{137}Cs information. Liu et al. (2003) and Milne and Heimsath (2009) provided simple calculations to estimate SOC redistribution from erosion and deposition, so for this case, the SOC redistribution calculations were combined using Eq. (5):

$$SOC_{ED} = \frac{\left((soil_{ED} \times 100) \times \frac{\%SOC}{100} \times enrich\right)}{10} \tag{5}$$

where SOC_{ED} is the redistributed SOC (g C m^{-2} yr^{-1}); $soil_{ED}$ is the estimated soil erosion and deposition from water and tillage erosion (t ha^{-1} yr^{-1}), multiplied by 100 to convert units to g m^{-2} yr^{-1}; *% SOC* is the SOC content percentage from Ritchie et al. (2007); and *enrich* is an enrichment factor expressed as the ratio of SOC concentration in the eroded soil to that in the topsoil layer for the study area (Liu et al., 2003). The SOC content percentage used in this study was interpolated spatially using Surfer software algorithms from locations and SOC measurements made on the ^{137}Cs samples (Ritchie et al., 2007).

3. Results and discussion

3.1. DEM spatial resolution effects in soil erosion and deposition

In the USPED model, water erosion in a DEM cell is dependent on the surface runoff in that cell, which in turn depends on the upstream contribution area; this upstream contribution area generates the erosion network calculated as the convergence of the sediment flow, and the deposition network is obtained by alteration in the sediment transport capacity (Oliveira et al., 2013). Some previous studies have used a 10-m DEM because it is a rational compromise between grid size resolution, data volume, and computing time needed to use hydrological process modeling to simulate erosion changes when conservation practices are implemented at different scales (Mitasova et al., 1999; Tamene and Vlek, 2007). Other studies have observed that DEM spatial resolution between 2 m and 20 m provided reasonable results for soil erosion analysis (Warren et al., 2000, 2005). An interaction is expected between the grid scale in the DEM and the appropriate values of the parameters calibrated to a particular area (Quinn et al., 1991). Table 3 shows the

Table 2
Input settings used in field site 2.

Input	Value	Units	Source
R factor	150	$\frac{\text{hundreds of ft}-\text{tonf}\cdot\text{in}}{\text{acre}\cdot\text{hr}\cdot\text{yr}}$	Schumacher et al. (2005)
K factor	0.24–0.32	$\frac{\text{ton}\cdot\text{acre}\cdot\text{hr}}{\text{hundreds of acre}\cdot\text{ft}-\text{tonf}\cdot\text{in}}$	SSURGO (USDA NRCS, 2012)
C factor	0.31	Dimensionless	Schumacher et al. (2005)
P factor	1	Dimensionless	Schumacher et al. (2005)
k-till	718	kg m^{-1} yr^{-1}	Schumacher et al. (2005)
DEM	314.58 ± 1.04	m (original spatial resolution 2 m)	Kaspar et al. (2004)
m	1.0–1.6	Dimensionless	Mitasova and Mitas (2001)
n	1.0–1.3	Dimensionless	Mitasova and Mitas (2001)
SOC content	2.34 ± 0.88	Percentage	Ritchie et al. (2007)

DEM: digital elevation model, SOC: soil organic carbon. Value information for DEM and SOC content include mean and standard deviation.

Table 3
Statistic results from different DEM spatial resolutions compared with observed information using the recommended topographic exponents: m rill = 1.6, n rill = 1.3, m sheet = 1.0, and n sheet = 1.0.

	R^2	RMSE	PBias	NSE	RSR	Min	Max	Mean	Stdev
Field site 1									
DEM 10 m	0.42	26.3	−87.8	0.4	0.8	−59.3	89.7	0.4	19.6
DEM 24 m	0.61	24.5	−134.1	0.5	0.7	−27.9	66.3	−1.1	15.5
DEM 30 m	0.50	25.8	−135.4	0.4	0.8	−32.5	64.0	−1.1	16.3
DEM 56 m	0.33	29.5	−180.1	0.3	0.9	−18.2	44.5	−2.6	13.1
Field site 2									
DEM 10 m	0.34	20.2	−80.6	0.1	0.9	−58.9	63.7	−0.9	22.0
DEM 24 m	0.49	17.3	−119.6	0.4	0.8	−32.2	60.0	0.9	20.9
DEM 30 m	0.42	19.1	−139.9	0.2	0.9	−26.5	57.2	1.8	21.3
DEM 56 m	0.38	19.0	−117.6	0.2	0.9	−29.8	45.1	0.8	19.9

R^2: R square, RMSE: root mean square error, PBias: percent bias, NSE: Nash–Sutcliffe efficiency, RSR: ratio of the root mean square error to the standard deviation of measured data, Min: minimum, Max: maximum, and Stdev: standard deviation.

results from the DEM spatial resolution analysis using aggregated 10-m, 24-m, 30-m, and 56-m DEMs to estimate soil redistribution from water and tillage. These results show that the aggregated 24-m DEM provided the best fit in the two field study areas when they were compared with the ^{137}Cs soil redistribution information. The 24-m results predicted soil erosion and deposition with $R^2 = 0.61$ for field site 1 and $R^2 = 0.49$ for field site 2 when using the default values of the m and n exponents ($m = 1.6$ and $n = 1.3$ for prevailing rill erosion and $m = 1.0$ and $n = 1.0$ for sheet erosion) recommended by Mitasova and Mitas (2001). The linear regression equations between the simulated and observed information were statistically significant in both cases ($p < 0.05$) using ANOVA. In addition, the overall performance using the aggregated 24-m DEM provided unsatisfactory simulation trends (NSE = 0.5), satisfactory simulation of residual variation (RSR = 0.7), and overestimation model bias (PBIAS = −137.5) in field site 1, but unsatisfactory results for the three measurements (NSE = 0.3, RSR = 0.8, and PBIAS = −119.2) in field site 2. These initial analysis results based on the DEM cell size have two possible causes: (1) the cell size is close to the grid-point sample spacing of about 25 m used for the ^{137}Cs measurements in the field sites (Ritchie et al., 2007) or (2) this resolution was closer to the 22.4-m slope length used in the derivation of the topographic factors for USLE, from which the USPED model is derived (Oliveira et al., 2013). The overall performance results could occur because we focused the analysis just on DEM cell size while other erosion factors, such as the rainfall erosivity, soil erodibility, and topographic cover management factors, were constant, so additional work can be applied to improve the current results.

3.2. Model results from calibration to validate the model framework

Based on the previous results, the 24-m aggregated DEM was used for the calibration process for the m (1.0–1.6) and n (1.3–1.0)

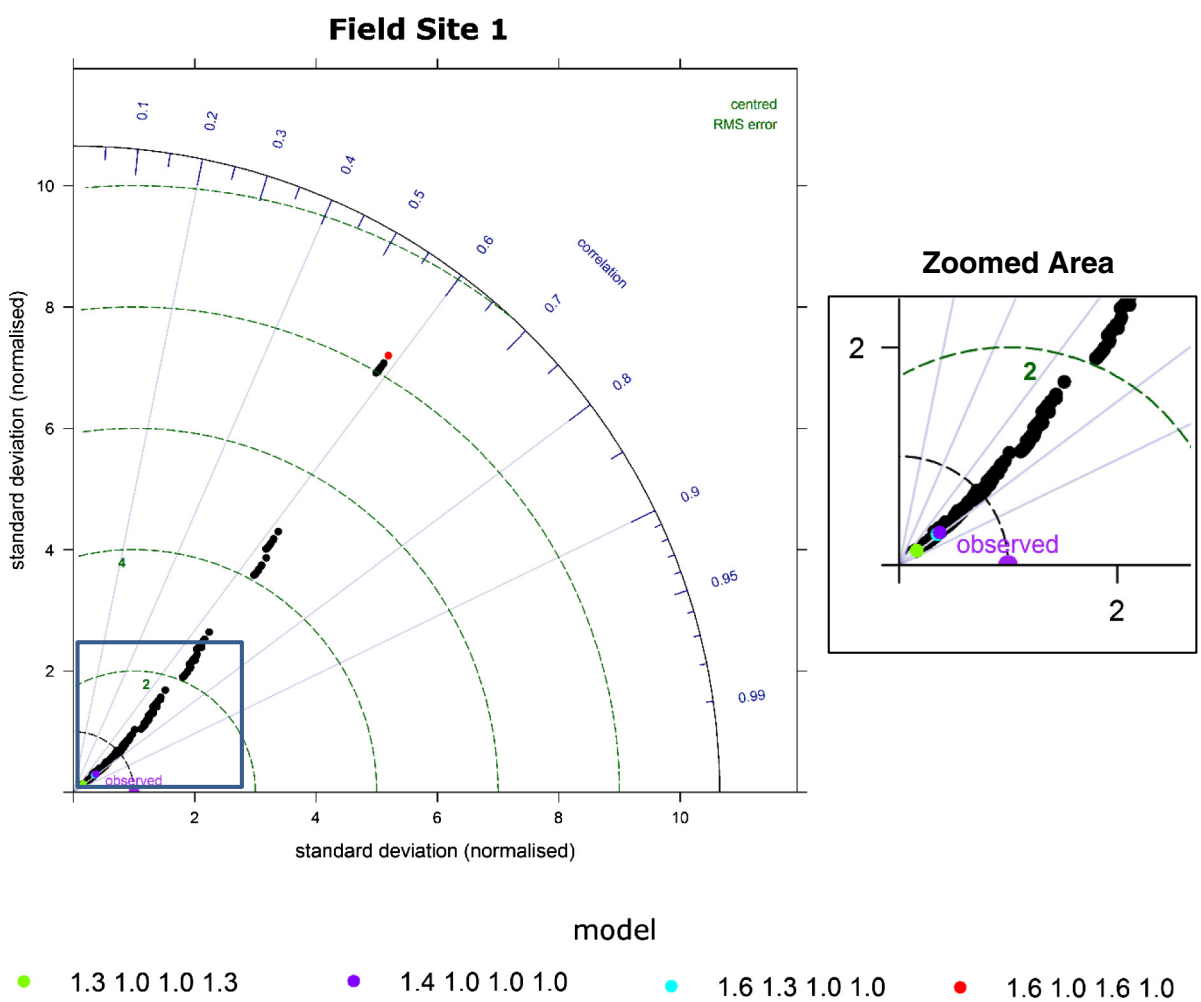

Fig. 4. Calibration of the upslope contributing area parameters in the model framework, where $m = 1.0$–1.6 and $n = 1.0$–1.3 for rill and sheet erosion in field site 1. Black dots represent the combinations of the topographic parameters defined for every 0.1 increase in these parameters.

Table 4
Statistics analysis results for Iowa field 1 (n = 224).

Field site 1	R^2	RMSE	PBias	NSE	RSR	Min	Max	Mean	Stdev
^{137}Cs estimated soil erosion/deposition						−89.8	172.6	3.2	34.3
m rill 1.3, n rill 1.0, m sheet 1.0, n sheet 1.3	0.60	29.32	−110.5	0.27	0.85	−22.7	23.9	−0.3	7.1
m rill 1.4, n rill 1.0, m sheet 1.0, n sheet 1.0	0.61	24.14	−137.5	0.50	0.70	−28.9	72.9	−1.2	16.4
m rill 1.6, n rill 1.0, m sheet 1.6, n sheet 1.0	0.34	287.70	−1129.2	−69.5	8.38	−747.8	1989.4	−33.1	304.8
m rill 1.6, n rill 1.3, m sheet 1.0, n sheet 1.0	0.61	24.51	−134.1	0.49	0.71	−27.9	66.3	−1.1	15.5

R^2: R-square, RMSE: root mean square error, PBias: percent bias, NSE: Nash–Sutcliffe efficiency, RSR: ratio of the root mean square error to the standard deviation of measured data, Min: minimum, Max: maximum, and Stdev: standard deviation.

exponents, where variability of these exponents was calculated based on the percent of slope, resulting in about 784 simulations for field site 1. The Taylor Diagram summarizes how closely a set of patterns matches observations in terms of correlation, centered RMSE, and the amplitude of variations by the standard deviation (Taylor, 2001). Fig. 4 shows the Taylor Diagram for field site 1, where the different simulations for each of the combinations of the exponents are represented in black, and the selected parameter combinations that showed the best and worst results, based on the three model performance statistics, are in color. In this case, the purple and cyan dots overlay because of the same $R^2 = 0.61$ and close RMSE values (24.14 and 24.51 t ha^{-1} yr^{-1}). Close to these two dots, the green dot can be found with $R^2 = 0.60$. On the other hand, the red dot shows the worst fit with $R^2 = 0.34$. In addition, Table 4 shows the statistical summary of selected combinations of parameters, where the highest statistically significant linear association was found when using $m = 1.4$ and $n = 1.0$ for prevailing rill erosion, and $m = 1.0$ and $n = 1.0$ for prevailing sheet erosion in field site 1 with $R^2 = 0.61$, r = 0.78, and $p < 0.05$. Based on the calibration process for field site 1, the model framework topographic exponents from field site 1 were validated using field site 2. Table 5 shows the statistical summary with $R^2 = 0.49$, r = 0.70, and $p < 0.05$ for the calibrated topographic parameters from field site 2. Moreover, these tables show that the overall performance did not improve when using the calibrated topographic exponents for rill erosion and sheet erosion. Fig. 5 shows the linear associations between the observed and simulation information for field site 1 (a) and field site 2 (b) using scatterplots along with their coefficient of determination ($R2 = R^2$) for $m = 1.4$ and $n = 1.0$ for prevailing rill erosion, and $m = 1.0$ and $n = 1.0$ for prevailing sheet erosion.

3.3. Spatial patterns in soil erosion and deposition from water and tillage erosion

Spatial distributions of simulated total (water + tillage) and ^{137}Cs-derived soil redistribution are shown in Fig. 6 for both sites, along with ^{137}Cs sampling points and DEM-derived contour lines and hillshade. The total erosion derived from the ^{137}Cs measurements in Fig. 6 (c and d) includes all types of erosion processes, such as water, wind, and tillage. The ^{137}Cs soil redistribution surface map was derived using regularized spline spatial interpolation in ArcGIS and the sampling points ($n = 224$ for field site 1 and $n = 134$ for field site 2). For this study, the comparison was made only between ^{137}Cs soil redistribution and the model estimates from water and tillage erosion. The simulated total soil erosion and deposition showed high erosion in the top elevation and hillslope areas whereas deposition occurred in the lower elevation areas. Similar spatial patterns over the landscape on the two fields were found between the simulated and the observed soil redistributions (surface and sampling points); however, there are differences between them. For example, the ^{137}Cs soil redistribution map shows larger areas with the highest erosion and deposition rate

Table 5
Statistics analysis results for Iowa field 2 (n = 134).

Field site 2	R^2	RMSE	PBias	NSE	RSR	Min	Max	Mean	Stdev
^{137}Cs estimated soil erosion/deposition						−53.5	58.1	−4.5	21.7
m rill 1.4, n rill 1.0, m sheet 1.0, n sheet 1.0	0.49	17.75	−119.2	0.3	0.8	−32.8	63.8	0.9	21.9
m rill 1.6, n rill 1.3, m sheet 1.0, n sheet 1.0	0.49	17.31	−119.6	0.4	0.8	−32.2	60.0	0.9	20.9

R^2: R-square, RMSE: root mean square error, PBias: percent bias, NSE: Nash–Sutcliffe efficiency, RSR: ratio of the root mean square error to the standard deviation of measured data, Min: minimum, Max: maximum, and Stdev: standard deviation.

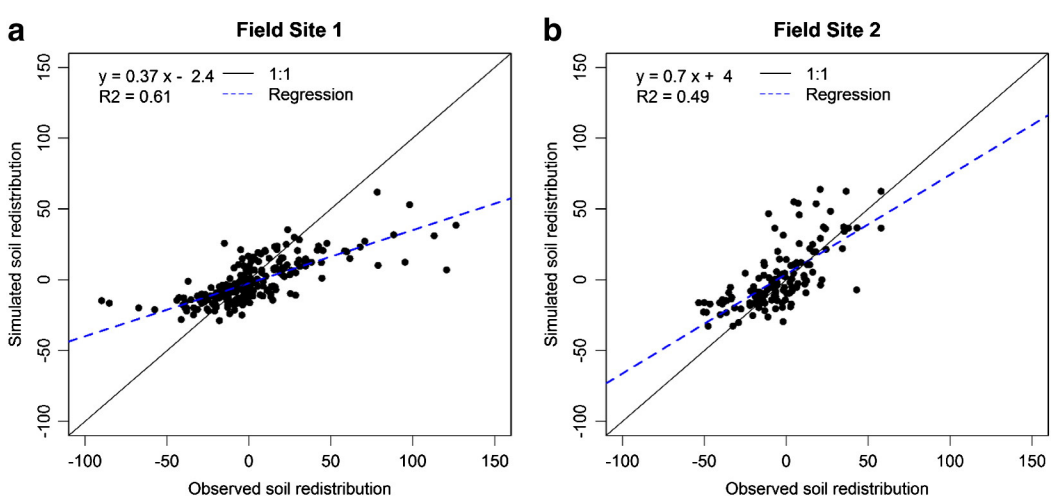

Fig. 5. Comparison of the simulated and observed soil redistributions in field site 1 (a) and field site 2 (b).

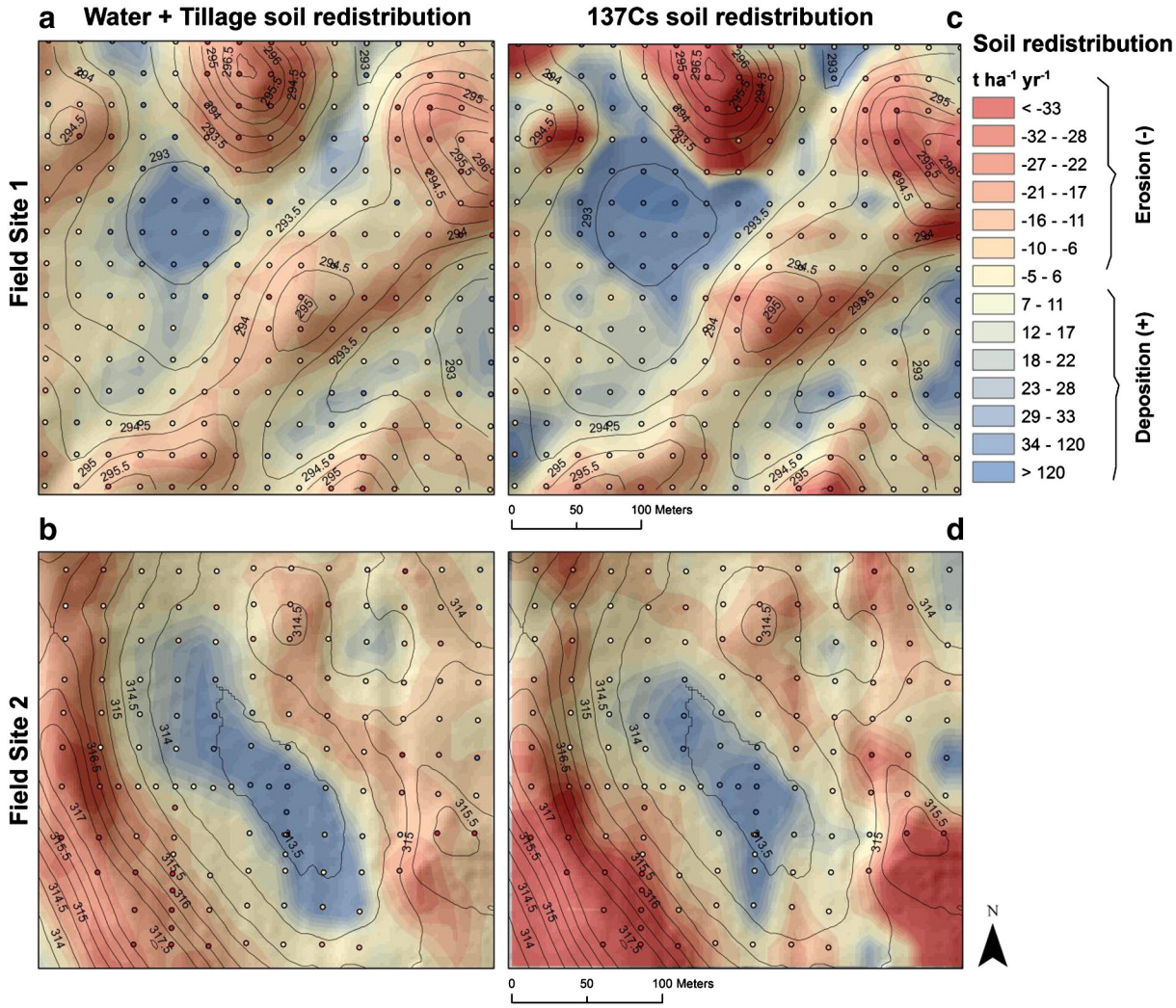

Fig. 6. Soil redistribution from simulated water and tillage (a and b) and interpolated ^{137}Cs estimates (c and d) along with DEM-derived contour lines and hillshade, and ^{137}Cs sampling points for field site 1 (a and c) and field site 2 (b and d).

classes than the simulated results. Schumacher et al. (2005) discussed that some of the differences can be attributed to the effect of water ponding, overland water flow onto the field sites from outside of the field boundaries, and modeling limitations. In addition, another difference between the estimates can be related to the dynamic landscape and topographic changes that can occur over time. For example, the ^{137}Cs measurements imply that the topography in the late 1950s and early 1960s was different with higher and steeper hills and lower and larger depressions. In addition, the ^{137}Cs measurements also suggest that the erosivity of soil on the summit and shoulders probably decreased over time as subsoil was exposed. For both sites, we assumed that field areas with high elevation and slope greater than 3.5% had high erosion rates, whereas areas with low elevation and slope less than or equal to 1% had high deposition rates. Tables 6 and 7 show the mean and standard deviation for soil redistribution between simulated and observed information for field site 1 and field site 2, respectively. In both cases, net deposition was found in areas with slopes less than or equal to 1% and net erosion in areas with slopes greater than 3.5%. In addition, field site 2 had the steepest areas (with slope greater than 5%) where simulated results showed higher estimated erosion rates than the ^{137}Cs information. Ritchie et al. (2007) postulated that the change in pattern for soil redistribution from the ^{137}Cs information for slopes greater than 4% may be a statistical anomaly because of a limited number of grid cells in that slope category and the way Surfer's algorithms, which were used to generate grid maps, calculate grid cell values for edge grid cells.

Fig. 7 shows the relationship between slope percentage with ^{137}Cs and simulated soil redistribution for (a) field site 1 and (b) field site 2. In this figure, patterns of soil redistribution from observed and simulated were similar; however, in field site 1 for low slope areas the ^{137}Cs measurements were higher than the model predictions, and this could have happened because of the water ponding and the off-site effects

Table 6
Mean and standard deviation for soil and SOC redistribution from ^{137}Cs and simulated results in field site 1. Negative values indicate erosion while positive values indicate deposition.

Slope (%)	Number of sample points	^{137}Cs soil redistribution rates (t ha^{-1} yr^{-1})	water + tillage soil redistribution rates (t ha^{-1} yr^{-1})	Estimated soil organic carbon (SOC) (g C m^{-2} yr^{-1})
Slope ≤ 1	49	32.8 ± 47.6	15.4 ± 19.4	10.2 ± 14.9
1 < slope ≤ 3.5	157	−2.2 ± 21.7	−4.3 ± 11.5	−1.0 ± 6.0
3.5 < slope ≤ 5	18	−30.0 ± 24.6	−19.1 ± 5.2	−2.8 ± 2.3
All	224	3.2 ± 34.3	−1.2 ± 16.4	1.3 ± 9.8

Table 7
Mean and standard deviation for soil and SOC redistribution from ^{137}Cs and simulated results in field site 2. Negative values indicate erosion while positive values indicate deposition.

Slope (%)	Number of sample points	^{137}Cs soil redistribution rates (t ha^{-1} yr^{-1})	water + tillage soil redistribution rates (t ha^{-1} yr^{-1})	Estimated soil organic carbon (SOC) (g C m^{-2} yr^{-1})
Slope ≤ 1	43	6.7 ± 24.6	12.4 ± 26.1	11.8 ± 19.7
1 < slope ≤ 3.5	71	−7 ± 17.1	−1.6 ± 17.2	0.8 ± 8.9
3.5 < slope ≤ 5	18	−21.3 ± 17.6	−14.1 ± 10.5	−4.0 ± 3.3
Slope > 5	2	−4.2 ± 2.3	−25.1 ± 4.6	−8.3 ± 1.5
All	134	−4.5 ± 21.7	0.9 ± 21.8	3.6 ± 14.3

mentioned previously. A comparison of the percentage of erosion and deposition areas over the landscape in field site 1 showed that 56% of the sampling points from the ^{137}Cs soil measurements were from eroded areas, whereas the simulation model estimated that 63% of the points were in eroded areas. Similarly, in field site 2, the ^{137}Cs soil measurements showed that 62% of the sampling points were in eroded areas, and the model estimated that 60% of the points were in eroded areas. Additionally, for field site 1, both ^{137}Cs soil measurements and the model simulation showed that 31% of the sampling points had erosion rates that exceeded the soil tolerance limit (T) of 11 t ha^{-1} yr^{-1} (5 t ac^{-1} yr^{-1}), which is similar to the 36% estimated by Schumacher et al. (2005). In field site 2, the ^{137}Cs soil measurements showed that 37% of the sampled areas exceeded the T value while the model estimated 35%. In both cases, the simulated results showed similar eroded areas to the observed information.

Additional analysis was applied using the soil redistribution from ^{137}Cs and the simulated soil redistribution to test for differences between the ^{137}Cs and simulated means in each field site. First, a Shapiro–Wilk test was applied to both estimates using the sampling point information to test the normality. The results showed that both simulated and observed datasets were not normally distributed for field site 1 ($p < 0.05$), but for field site 2, the ^{137}Cs data were normally distributed ($p = 0.1377$) while the simulated results were not normally distributed ($p < 0.05$). Based on these results, the Wilcoxon signed-ranked test, a non-parametric statistical method, was applied in each field to determine if both estimates differed significantly in each field. The results showed that the means from the simulated and observed estimates were not significantly different in field site 1 (W = 23,810.5, $p = 0.3513$) or in field site 2 (W = 9574.5, $p = 0.23475$).

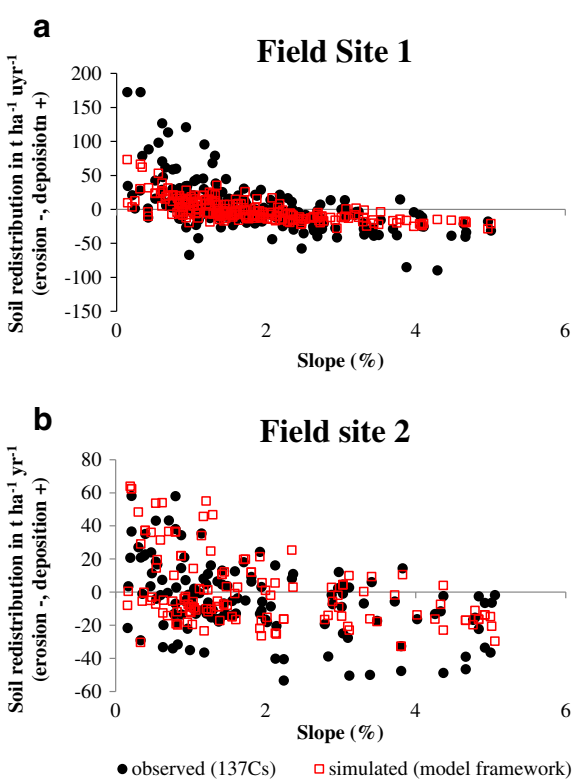

Fig. 7. Relationships between observed (^{137}Cs) and simulated (USPED + TEP) erosion (negative) and deposition (positive) by slope percentage in field site 1 (a) and in field site 2 (b).

3.4. SOC redistribution from water and tillage soil erosion and deposition

Simulated soil redistribution rates, SOC content (%) from the ^{137}Cs measurements, and an enrichment factor of 2.0 (*enrich* = 2.0) were used to estimate SOC redistribution in both sites based on Eq. (5). Fig. 8 shows the spatial pattern of SOC redistribution on the landscape of field site 1 (c) and of field site 2 (d). Tables 6 and 7 show the mean and standard deviation of the simulated SOC redistribution for all the sampling points and by slope percentage ranges for field site 1 and field site 2, respectively. Averaged over the entire field, SOC redistribution was 1.3 ± 9.8 g C m^{-2} yr^{-1} and 3.6 ± 14.3 g C m^{-2} yr^{-1} for field sites 1 and 2, respectively. Spatial distribution patterns and summary information by slope percent ranges showed SOC loss (negative values) in the eroded areas and SOC gain (positive value) in the deposition areas, so soil loss increases and SOC decreases as slope in the fields increases. On the other hand, in the lower elevation areas where percent slope is less than or equal to 1 (slope ≤ 1%), there were high deposition values for both soil and SOC. The results of this study were similar to other studies that have shown that reduction of SOC occurred in upland eroded areas, and this eroded SOC was added to deposition areas (Liu et al., 2003; Ritchie et al., 2007; Smith et al., 2005).

4. Conclusions

In this study, a model framework that included the USPED and TEP models was used to estimate soil erosion and deposition from water and tillage processes. The results from this model framework provided information on the spatial estimates of soil and SOC redistribution by water and tillage erosion in two agricultural fields in Iowa. The model framework was evaluated for different DEM spatial resolutions (10-m, 24-m, 30-m, and 56-m) and topographic exponents ($m = 1.0$–1.6 and $n = 1.0$–1.3) using soil redistribution rates from ^{137}Cs measurements. First, the DEM spatial resolution evaluation showed that the aggregated 24-m DEM provided the best fit in the two field study areas (field sites 1 and 2). Second, the topographic exponents evaluation showed that $m = 1.4$ and $n = 1.0$ for rill erosion, and $m = 1.0$ and $n = 1.0$ for sheet erosion, provided the best fit with the ^{137}Cs data at both field sites. Spatial patterns between the simulated and observed soil redistributions were similar over the landscape on the two field sites; however, some differences were found that could be related to model limitations and to the effect of the dynamics of hydrology and topography on the landscape. The estimated soil redistribution rates from each field site were used to calculate SOC redistribution on the landscape. The results showed where carbon loss and gain occurred because of soil erosion and deposition from water and tillage erosion. Spatial distribution patterns showed SOC loss (negative values) in the eroded areas and SOC gain (positive value) in the deposition areas. Estimated average SOC redistributions were 1.3 ± 9.8 g C m^{-2} yr^{-1} in field site 1 and 3.6 ± 14.3 g C m

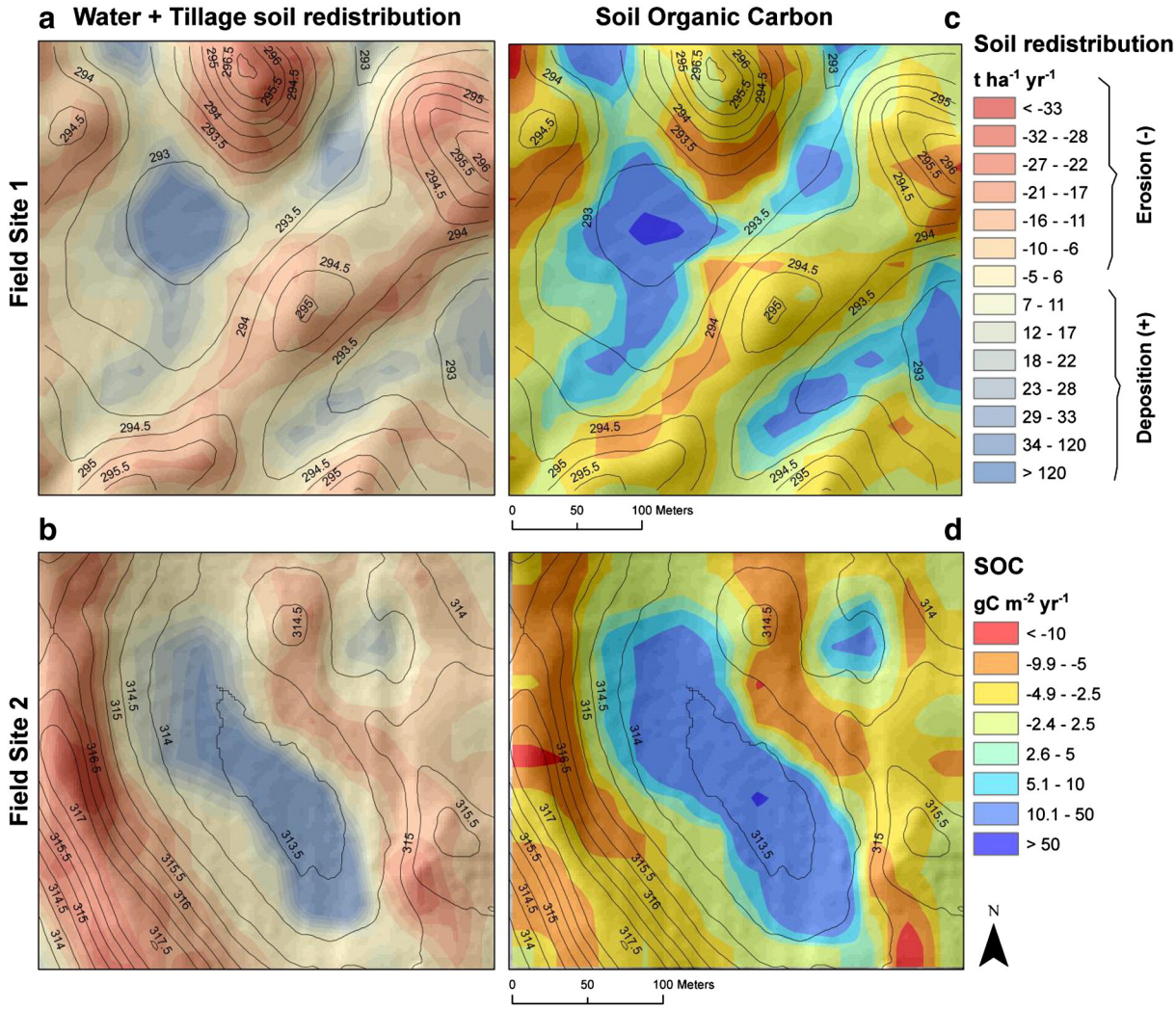

Fig. 8. Simulated soil (a and b) and SOC (c and d) redistribution from water and tillage in field site 1 (a and c) and field site 2 (b and d).

$^{-2}$ yr^{-1} in field site 2. Therefore, this study demonstrated the importance of the spatial resolution and the topographic exponents to estimate and map soil redistribution and the SOC dynamics throughout the landscape, helping to identify places where erosion and deposition by water and tillage are occurring at high rates. Additional work is needed to improve the current results for these sites by better characterizing the rainfall erosivity and cover management factors and by considering the effect of changes in topography over time caused by erosion and deposition. Future work also would include applying the model framework over larger agricultural areas. Improving predictions about soil erosion and deposition in agricultural landscapes and assessing their impacts on soil carbon redistribution and dynamics may help to understand where and why soil and SOC redistribution is happening. This improved understanding may lead to better management to control erosion in the future and better assessments of the impact of erosion and deposition on C loss and sequestration at local or regional scales through SOC redistribution.

Acknowledgments

This study was part of the USGS Land Carbon project. The work of C.J. Young (ERT, Inc.) was performed under USGS contract G10PC00044. We thank Yiping Wu for an internal review of this manuscript and for providing some suggestions for improvement. We also thank Thomas Adamson for editing the document to improve English usage and grammar. Any use of trade, firm, or product names is for descriptive purposes only and does not imply endorsement by the U.S. Government.

Appendix A. Supplementary data

Supplementary data associated with this article can be found in the online version, at http://dx.doi.org/10.1016/j.geoderma.2014.05.019. These data include Google map of the most important areas described in this article.

References

Al-Smadi, M.A., 2007. Areal Modeling of Erosion for Environmental Nonpoint Applications (AMEENA). (PhD dissertation Thesis) Virginia Polytechnic Institute and State University.

Arriaga, F., Lowery, B., 2007. Erosion and productivity. In: Trimble, S.W. (Ed.), Encyclopedia of water science. CRC Press, Boca Raton, FL, pp. 262–264.

Blanco, H., Lal, R., 2008. Soil and water conservation. Principles of soil conservation and management. Springer, Netherlands, pp. 1–19.

Brady, N.C., Weil, R.R., 2008. The nature and properties of soils. Prentice Hall, Upper Saddle River, NJ.

Claessens, L., Heuvelink, G., Schoorl, J., Veldkamp, A., 2005. DEM resolution effects on shallow landslide hazard and soil redistribution modelling. Earth Surf. Process. Landf. 30 (4), 461–477.

Colvin, T., Jaynes, D., Karlen, D., Laird, D., Ambuel, J., 1997. Yield variability within a central Iowa field. Trans. ASAE 40 (4), 883–889.

Esri, 2011. ArcGIS desktop: release 10. Environmental Systems Research Institute, Redlands, CA.

Fang, H., Li, Q., Sun, L., Cai, Q., 2012. Using 137Cs to study spatial patterns of soil erosion and soil organic carbon (SOC) in an agricultural catchment of the typical black soil region, Northeast China. J. Environ. Radioact. 112, 125–132.
Flanagan, D.C., 2007. Erosion, encyclopedia of soil science, Second edition. Taylor & Francis, pp. 523–526.
Fornes, W.L., Whiting, P.J., Wilson, C.G., Matisoff, G., 2005. Caesium-137-derived erosion rates in an agricultural setting: the effects of model assumptions and management practices. Earth Surf. Process. Landf. 30 (9), 1181–1189.
Foster, G.R., McCool, D.K., Renard, K.G., Moldenhauer, W.C., 1981. Conversion of the universal soil loss equation to SI metric units. J. Soil Water Conserv. 36 (6), 355–359.
Garcia Rodriguez, J.L., Gimenez Suarez, M.C., 2012. Methodology for estimating the topographic factor LS of RUSLE3D and USPED using GIS. Geomorphology 175–176, 98–106.
Harden, J.W., Berhe, A.A., Torn, M., Harte, J., Liu, S., Stallard, R.F., 2008. Soil erosion: data say C sink. Science 320 (5873), 178–179.
Ito, A., 2007. Simulated impacts of climate and land-cover change on soil erosion and implication for the carbon cycle, 1901 to 2100. Geophys. Res. Lett. 34 (9), L09403.
Jacinthe, P., Lal, R., 2007. Erosion and carbon dioxide, encyclopedia of soil science, Second edition. Taylor & Francis, pp. 527–531.
Jaynes, D.B., Kaspar, T.C., Colvin, T.S., 2011. Economically optimal nitrogen rates of corn: management zones delineated from soil and terrain attributes. Agron. J. 103 (4), 1026–1035.
Jetten, V.G., Maneta, M.P., 2010. Calibration of erosion models. Handbook of erosion modelling. John Wiley & Sons, Ltd, Chichester, UK, pp. 33–51.
Karlen, D., Colvin, T., 1992. Alternative farming system effects on profile nitrogen concentrations on two Iowa farms. Soil Sci. Soc. Am. J. 56 (4), 1249–1256.
Kaspar, T.C., Pulido, D.J., Fenton, T.E., Colvin, T.S., Karlen, D.L., Jaynes, D.B., Meek, D.W., 2004. Relationship of corn and soybean yield to soil and terrain properties. Agron. J. 96 (3), 700–709.
Lal, R., 1998. Potential of United States cropland to sequester carbon and mitigate the greenhouse effect. Ann Arbor Press, Chelsea, MI.
Lal, R., 2002. Soil carbon dynamics in cropland and rangeland. Environ. Pollut. 116 (3), 353–362.
Lal, R., 2003. Soil erosion and the global carbon budget. Environ. Int. 29 (4), 437–450.
Lal, R., Pimentel, D., 2008. Soil erosion: a carbon sink or source? Science 319 (5866), 1040–1042.
Leh, M., Bajwa, S., Chaubey, I., 2011. Impact of land use change on erosion risk: an integrated remote sensing, geographic information system and modeling methodology. Land Degrad. Dev. 24 (5), 409–421.
Lindstrom, M.J., 2007. Tillage erosion: description and process, encyclopedia of soil science, Second edition. Taylor & Francis, pp. 1776–1778.
Lindstrom, M.J., Schumacher, J.A., Schumacher, T.E., 2000. TEP: a Tillage Erosion Prediction model to calculate soil translocation rates from tillage. J. Soil Water Conserv. 55 (1), 105–108.
Liu, S., Bliss, N., Sundquist, E., Huntington, T.G., 2003. Modeling carbon dynamics in vegetation and soil under the impact of soil erosion and deposition. Global Biogeochem. Cycles 17 (2), 1074.
Liu, J., Liu, S., Tieszen, L.L., Chen, M., 2007. Estimating soil erosion using the USPED model and consecutive remotely sensed land cover observations. Proceedings of the 2007 summer computer simulation conference. Society for Computer Simulation International, San Diego, California.
McCarty, G.W., Ritchie, J.C., 2002. Impact of soil movement on carbon sequestration in agricultural ecosystems. Environ. Pollut. 116 (3), 423–430.
Milne, E., Heimsath, A., 2009. Soil organic carbon. In: Cleveland, C.J. (Ed.), Encyclopedia of earth. Environmental Information Coalition, National Council for Science and the Environment, Washington, D.C.
Mitas, L., Mitasova, H., 1998. Distributed soil erosion simulation for effective erosion prevention. Water Resour. Res. 34 (3), 505–516.
Mitasova, H., Mitas, L., 2001. Multiscale soil erosion simulations for land use management. In: Harmon, R., Doe, W. (Eds.), Landscape erosion and landscape evolution modeling. Kluwer Academic/Plenum, New York, pp. 321–347.
Mitasova, H., Hofierka, J., Zlocha, M., Iverson, R., 1996. Modeling topographic potential for erosion and deposition using GIS. Int. J. Geogr. Inf. Syst. 10 (5), 629–641.
Mitasova, H., Mitas, L., Brown, W.M., Johnston, D., 1999. Terrain modeling and soil erosion simulations for Fort Hood and Fort Polk test areas. University of Illinois, Urbana-Champaign, IL.
Morgan, R.P.C., 2010. Model development: a user's perspective. Handbook of erosion modelling. John Wiley & Sons, Ltd, Chichester, UK, pp. 7–32.
Moriasi, D., Arnold, J., Van Liew, M., Bingner, R., Harmel, R., Veith, T., 2007. Model evaluation guidelines for systematic quantification of accuracy in watershed simulations. Trans. ASABE 50 (3), 885–900.
Nearing, M., Lane, L., Lopes, V.L., 1994. Modeling soil erosion. In: Lal, R. (Ed.), Soil erosion research methods. St. Lucie Press, Delray Beach, FL, pp. 127–156.
Nelson, R.G., 2002. Resource assessment and removal analysis for corn stover and wheat straw in the Eastern and Midwestern United States—rainfall and wind-induced soil erosion methodology. Biomass Bioenergy 22 (5), 349–363.
Oliveira, A.H., da Silva, M.A., Silva, M.L.N., Curi, N., Neto, G.K., de Freitas, D.A.F., 2013. Development of topographic factor modeling for application in soil erosion models. In: Hernandez Soriano, M.C. (Ed.), Soil processes and current trends in quality assessment. InTech, Rijeka, Croatia.
Olson, K.R., 2013. Soil organic carbon sequestration, storage, retention and loss in U.S. croplands: issues paper for protocol development. Geoderma 195–196, 201–206.
Pimentel, D., 2006. Soil erosion: a food and environmental threat. Environ. Dev. Sustain. 8 (1), 119–137.
Pimentel, D., Harvey, C., Resosudarmo, P., Sinclair, K., Kurz, D., McNair, M., Crist, S., Shpritz, L., Fitton, L., Saffouri, R., 1995. Environmental and economic costs of soil erosion and conservation benefits. Science 267 (5201), 1117–1123.
Quinn, P., Beven, K., Chevallier, P., Planchon, O., 1991. The prediction of hillslope flow paths for distributed hydrological modelling using digital terrain models. Hydrol. Process. 5 (1), 59–79.
R Development Core Team, 2010. R: a language and environment for statistical computing. R Foundation for Statistical Computing, Vienna, Austria.
Ritchie, J.C., McHenry, J.R., 1990. Application of radioactive fallout cesium-137 for measuring soil erosion and sediment accumulation rates and patterns: a review. J. Environ. Qual. 19 (2), 215–233.
Ritchie, J.C., McCarty, G.W., Venteris, E.R., Kaspar, T.C., Owens, L., Slater, B.K., Nearing, M., Nichols, M.H., 2004. Assessing soil organic carbon redistribution with fallout 137Cesium. 13th International Soil Conservation Organization Conference (ISCO), Brisbane.
Ritchie, J.C., McCarty, G.W., Venteris, E.R., Kaspar, T.C., 2005. Using soil redistribution to understand soil organic carbon redistribution and budgets. In: Walling, D.E., Horowitz, A.J. (Eds.), Sediment budgets. IAHS Press, Wallingford, Oxfordshire, UK, pp. 3–8.
Ritchie, J.C., McCarty, G.W., Venteris, E.R., Kaspar, T.C., 2007. Soil and soil organic carbon redistribution on the landscape. Geomorphology 89 (1–2), 163–171.
Römkens, M.J.M., Helming, K., Prasad, S.N., 2002. Soil erosion under different rainfall intensities, surface roughness, and soil water regimes. Catena 46 (2–3), 103–123.
Schmidt, B., Ham, G., 1999. Foreword. In: Lal, R. (Ed.), Soil quality and soil erosion. Soil and Water Conservation Society, Ankeny, IA, pp. vii–ix.
Schoorl, J.M., Sonneveld, M.P.W., Veldkamp, A., 2000. Three-dimensional landscape process modelling: the effect of DEM resolution. Earth Surf. Process. Landf. 25 (9), 1025–1034.
Schumacher, T.E., 2007. Tillage erosion: properties and productivity effects, encyclopedia of soil science, Second edition. Taylor & Francis, pp. 1782–1784.
Schumacher, T., Lindstrom, M., Schumacher, J., Lemme, G., 1999. Modeling spatial variation in productivity due to tillage and water erosion. Soil Tillage Res. 51 (3), 331–339.
Schumacher, J.A., Kaspar, T.C., Ritchie, J.C., Schumacher, T.E., Karlen, D.L., Venteris, E.R., McCarty, G.W., Colvin, T.S., Jaynes, D.B., Lindstrom, M.J., Fenton, T.E., 2005. Identifying spatial patterns of erosion for use in precision conservation. J. Soil Water Conserv. 60 (6), 355–362.
Smith, S.V., Sleezer, R.O., Renwick, W.H., Buddemeier, R.W., 2005. Fates of eroded soil organic carbon: Mississippi basin case study. Ecol. Appl. 15 (6), 1929–1940.
Steinwand, A., Karlen, D., Fenton, T., 1996. An evaluation of soil survey crop yield interpretations for two central Iowa farms. J. Soil Water Conserv. 51 (1), 66–71.
Tallis, H.T., Ricketts, T., Guerry, A.D., Wood, S.A., Sharp, R., Nelson, E., Ennaanay, D., Wolny, S., Olwero, N., Vigerstol, K., Pennington, D., Mendoza, G., Aukema, J., Foster, J., Forrest, J., Cameron, D., Arkema, K., Lonsdorf, E., Kennedy, C., Verutes, G., Kim, C.K., Guannel, G., Papenfus, M., Toft, J., Marsik, M., Bernhardt, J., 2011. InVEST 2.4.5 user's guide. The Natural Capital Project, Stanford.
Tamene, L., Vlek, P.L.G., 2007. Assessing the potential of changing land use for reducing soil erosion and sediment yield of catchments: a case study in the highlands of northern Ethiopia. Soil Use Manag. 23 (1), 82–91.
Taylor, K.E., 2001. Summarizing multiple aspects of model performance in a single diagram. J. Geophys. Res. Atmos. 106 (D7), 7183–7192.
Toy, T.J., Foster, G.R., Renard, K.G., 2002. Introduction. Soil erosion: processes, prediction, measurement, and control. John Wiley & Sons, New York, pp. 1–23.
U.S. Department of Agriculture — Natural Resources Conservation Service, 1997. America's private land: a geography of hope.
U.S. Department of Agriculture — Natural Resources Conservation Service, 2012. Soil Survey Geographic (SSURGO) database
Van Oost, K., T.Quine, T., G.Govers, G., S.De Gryze, S., J.Six, J., J.Harden, J., J.Ritchie, J., G. McCarty, G., G.Heckrath, G., C.Kosmas, C., 2007. The impact of agricultural soil erosion on the global carbon cycleScience 318 (5850), 626–629.
Warren, S.D., Mitasova, H., Jourdan, M.R., Brown, W.M., Johnson, B.E., Johnston, D.M., Julien, P.V., Mitas, L., Molnar, D.K., Watson, C.C., 2000. Digital terrain modelling and distributed soil erosion simulation/measurement for minimizing environmental impacts of military training. Colorado Sate University, Fort Collins, CO.
S.D.Warren, S.D., H.Mitasova, H., M.G.Hohmann, M.G., S.Landsberger, S., F.Y.Iskander, F.Y., T.S.Ruzycki, T.S., G.M.Senseman, G.M., 2005. Validation of a 3-D enhancement of the Universal Soil Loss Equation for prediction of soil erosion and sediment depositionCatena 64 (2–3), 281–296.
Weaver, J.E., 1920. Root development in the grassland formation: a correlation of the root systems of native vegetation and crop plants. Carnegie Institution of Washington.
J.P.Wilson, J.P., M.S.Lorang, M.S., 2000. Spatial models of soil erosion and GISIn: Stewart, F. A., Michael, W. (Eds.), Spatial models and GIS: new potential and new models. Taylor & Francis, Philadelphia, PA, pp. 83–108.
Zhang, J.X., Wu, J.Q., Chang, K.-T., Elliot, W.J., Dun, S., 2009. Effects of DEM resolution and source on soil erosion modelling: a case study using the WEPP model. Int. J. Geogr. Inf. Sci. 22 (8), 925–942.